Materials Advances

ROYAL SOCIETY OF CHEMISTRY

PAPER

View Article Online
View Journal | View Issue

Cite this: *Mater. Adv.*, 2022, 3, 6335

One-pot route to fine-tuned hypercrosslinked polymer solid acid catalysts†

Alexander Blocher,‡ Florian Mayer, ‡ Paul Schweng, Teresa M. Tikovits, Neptun Yousefi and Robert T. Woodward *

Highly sulfonated polymers are promising heterogeneous catalysts due to their excellent chemical and thermal stability, as well as the possibility of employing low-cost synthesis routes. However, their production is time consuming and control of their chemical and physical properties is often difficult. We present sulfonated hypercrosslinked polymers produced using chlorosulfonic acid as a dual polymerisation catalyst and sulfonation agent, consolidating a conventional two-step process into a one-pot reaction. Network synthesis time is reduced from 5–6 days to <24 hours, while significantly lowering or eliminating the requirement of some reagents. These sulfonated networks display superior acid site densities and porosities compared to conventional equivalents and excellent control over polymer properties is achieved. The polymers are employed as heterogeneous acid catalysts in the hydrolysis of cyclohexyl acetate. Therein, it is shown that fine-tuning polymer properties has a dramatic effect on their catalytic performance, allowing the identification of key catalyst properties.

Received 1st April 2022,
Accepted 5th July 2022

DOI: 10.1039/d2ma00379a

rsc.li/materials-advances

Introduction

An increased demand for more sustainable approaches in the chemical industry is being driven by considerable socio-economic and environmental changes. As a result, reusable, energy efficient, and selective catalysts have become a key pillar in the principles of green chemistry.[1] By the immobilisation of homogeneous catalysts or equivalent chemical functionality onto inert insoluble frameworks, effective heterogeneous catalysts that adhere to these principles can be realised.[2] Heterogeneous catalysts offer advantages over homogeneous equivalents, such as use in continuous flow processes, simple separation and recovery from reactants and products, and straightforward recycling. However, reduced catalytic activities, high-costs, and poor stabilities can often hold-back the application of such catalysts in industry.[3] Immobilisation requires the synthesis of pre-functionalised frameworks, followed by the anchoring of active sites, often requiring multistep procedures and expensive reagents.[4] Moreover, immobilisation can alter the microenvironment of active sites, leading to decreased activity or poor accessibility for reactants. To make heterogeneous catalysts competitive with homogeneous equivalents, their active sites need to be dense and accessible, their production should exploit low-cost design, and their implementation has to offer simple operation and compatibility with many facets of modern catalysis.

Porous organic polymers (POPs) are excellent candidates for heterogeneous catalysis due to their high surface areas, tuneable textural properties, and excellent chemical, thermal, and mechanical stabilities. The vast number of synthetic routes to POPs also permit readily modifiable chemical functionality and/or broad bottom-up design. Common examples of POPs include covalent organic frameworks (COFs)[5] and conjugated microporous polymers (CMPs),[6] both of which have shown great potential in separation and catalysis applications. However, many POP synthesis routes require precious metal catalysts, which are typically not recycled, significantly driving up cost and hindering scale-up. Furthermore, specifically polymerisable groups in monomeric material are often required for the formation of POP networks. Such monomers are seldomly commercially available or are expensive.

Hypercrosslinked polymers (HCPs) are a low-cost class of POPs with excellent tunability.[7] HCPs are densely crosslinked amorphous networks, produced using simple Friedel–Crafts chemistry. One approach to HCPs utilises non-functional aromatic compounds (*i.e.* without specifically polymerisable groups) that are 'knitted' together in a variety of ways, such as using external crosslinkers,[8] solvent stitching reactions,[9] or Scholl reactions.[10,11] Another approach produces HCPs *via* self-condensation reactions of chloromethyl[12] or methyl ether[13] moieties with aromatic carbon to form crosslinks. Hypercrosslinking requires only abundant Fe- or Al-based Lewis acid catalysts[14] or simple organic acid catalysts.[15,16] Owing to their low costs and

Institute of Materials Chemistry and Research, Faculty of Chemistry, University of Vienna, Währinger Straße 42, 1090, Vienna, Austria.
E-mail: robert.woodward@univie.ac.at

† Electronic supplementary information (ESI) available. See DOI: https://doi.org/10.1039/d2ma00379a

‡ These authors contributed equally to this work.

broad design scope, HCPs are developed for a variety of applications including gas separation and storage,[17] solid state extraction,[18] and energy storage.[19] HCPs also show promise in heterogeneous catalysis, both as inert frameworks or as active materials.[20] HCP-based catalysts were employed for a wide array of transformations, ranging from biomass conversion[21,22] to the photocatalytic reduction of CO_2.[23,24] High surface areas allow for an abundance of catalytically active sites and hierarchically porous structures are beneficial to the mass transfer of reactants and products. As such, HCPs show excellent ability in catalysis and are ideal candidates for industrial applications in accordance with the principles of green chemistry.

Through treatment of HCPs with sulfonating agents, heterogeneous acid catalysts combining the desirable properties of HCPs with high acid-site densities, so called sulfonated HCPs (SHCPs), are produced. Dong *et al.* synthesised sulfonated hypercrosslinked benzene networks containing up to 2 mmol g^{-1} of SO_3H for the selective dehydration of D-(−)-fructose to 5-hydromethylfurfual, reaching conversions of >90%.[21] An analogous set of materials catalysed the selective conversion of carbohydrate substrates to ethyl levulinate in yields of up to 67%.[22] Therein, it was speculated that multiple variables, including surface area, catalyst dose, and acid density played a critical role in the efficiency of the catalytic transformation. Sulfonated carbazole-based HCPs with impressive SO_3H densities of 3.7 mmol g^{-1} were developed for the esterification of a number of fatty acids to produce biofuels, reaching conversions of up to 99%.[25] Elsewhere, a SHCP containing a phosphonium salt in its structure was used for the two-phase hydrolysis of cyclohexyl acetate to cyclohexanol, achieving conversions and selectivity of up to 93 and 95%, respectively.[26] SHCPs have also shown promise as selective adsorbents, including for propene/propane separation,[27,28] heavy metal adsorption,[29] and water pollutants.[30]

In conventional approaches, sulfonic acid groups are introduced *via* the post-synthetic treatment of HCPs using sulfonating agents, commonly chlorosulfonic acid. This route involves the swelling of the HCP network in inert solvent, followed by treatment with large excesses of the sulfonating agent. Although effective, control over the degree of sulfonation and the resulting porous properties of the catalyst is lacking. Furthermore, the approach is cumbersome, requiring the complete synthesis and work up of the HCP prior to sulfonation, resulting in a synthesis time of up to 6 days.

We present a strategy for the synthesis of SHCPs in a one-pot approach, significantly reducing reaction times and reagent use compared to conventional approaches. These SHCPs allow for careful catalyst design and have superior properties to SHCPs obtained using other synthetic procedures. Hazardous organic solvents and reagents are significantly reduced or eliminated altogether, making the method simple, safer, cleaner, and more economical. To assess the potential of these SHCPs as solid acid catalysts, we report their application to the hydrolysis of cyclohexyl acetate. The properties of these finely tuned SHCPs had a dramatic effect on their performance in this two-phase reaction, allowing for the identification of key catalyst properties for optimal catalytic performance.

Results and discussion

We synthesised ten SHCPs from 4,4′-bis(chloromethyl)biphenyl using chlorosulfonic acid as a dual polymerisation catalyst and sulfonation agent (a general reaction scheme is shown in Fig. 1a). Throughout the set, the ratio of chlorosulfonic acid to the aromatic monomer was varied to investigate the effect on the resulting SHCPs' textural and chemical properties. The progression from SHCP-1 to SHCP-10 follows an increasing catalyst-to-monomer ratio, precise values of which are given in Table 1. Briefly, 4,4′-bis(chloromethyl)biphenyl was dissolved in 1,2-dichloroethane (1,2-DCE) and cooled using an ice bath, after which a solution of chlorosulfonic acid in 1,2-DCE was added to initiate polymerisation. Upon formation of a solid, the mixture was sealed and heated at 80 °C for up to 22 h. The resulting solid was then washed with methanol before drying to yield the SHCP. More details are given in the ESI.† Including work up, the entire synthetic process reported herein is complete in under 48 h, representing a dramatic reduction from conventional approaches. In previous studies, polymer synthesis and work up required ~72 h for network formation prior to sulfonation, which is performed in a subsequent separate process requiring up to an additional 96 h.[27–29] Furthermore, by consolidating these steps into a one-pot process, we are able to significantly reduce solvent consumption and eliminate the need for both a discreet polymerisation catalyst and sulfonation agent. It is also worth noting that a shortened procedure in which heating time was reduced to 5 h showed no apparent detriment to resulting SHCP properties. Polymers were typically produced in yields of >90% when considering the incorporation of the acid catalyst as a sulfonic acid group. Networks ranged from a beige to dark brown colour with increasing catalyst to monomer ratios (Fig. S1, ESI†). All SHCPs were produced at least four times to ensure reproducibility.

We confirmed the successful formation of SHCPs using ^{13}C cross-polarisation/magic angle spinning solid-state NMR (CP/MAS ssNMR) (Fig. 1b). Signals at ~38 ppm are assigned to methylene bridges from newly formed crosslinks in all cases. A weak signal assigned to C–Cl at ~42 ppm can be seen in SHCP-1 and decreases in intensity through to SHCP-3, indicative of incomplete crosslinking due to low concentrations of chlorosulfonic acid. A signal at ~120 ppm is found in the shoulder of a larger peak in samples SHCP-5–SHCP-10, assigned to the C–S bond formed during sulfonation. At lower ratios of catalyst to monomer this peak can no longer be seen due to reduced degrees of sulfonation. All SHCPs showed strong signals at ~129 and ~139 ppm, corresponding to aromatic (C_{Ar}–H) and quaternary, or substituted, aromatic carbons (C_{Ar}–R), respectively. Although difficult to quantify due to overlapping peaks, it is clear that the ratio between substituted and unsubstituted aromatic peaks changes across the polymer set. Increasing amounts of chlorosulfonic acid in the initial formulation appear to increase the ratio of substituted to unsubstituted aromatic carbon. Considering the increase in C–S peak as well as the disappearance of the C–Cl peak with higher initial concentrations of chlorosulfonic acid, this is in line with expectation. We also confirmed successful

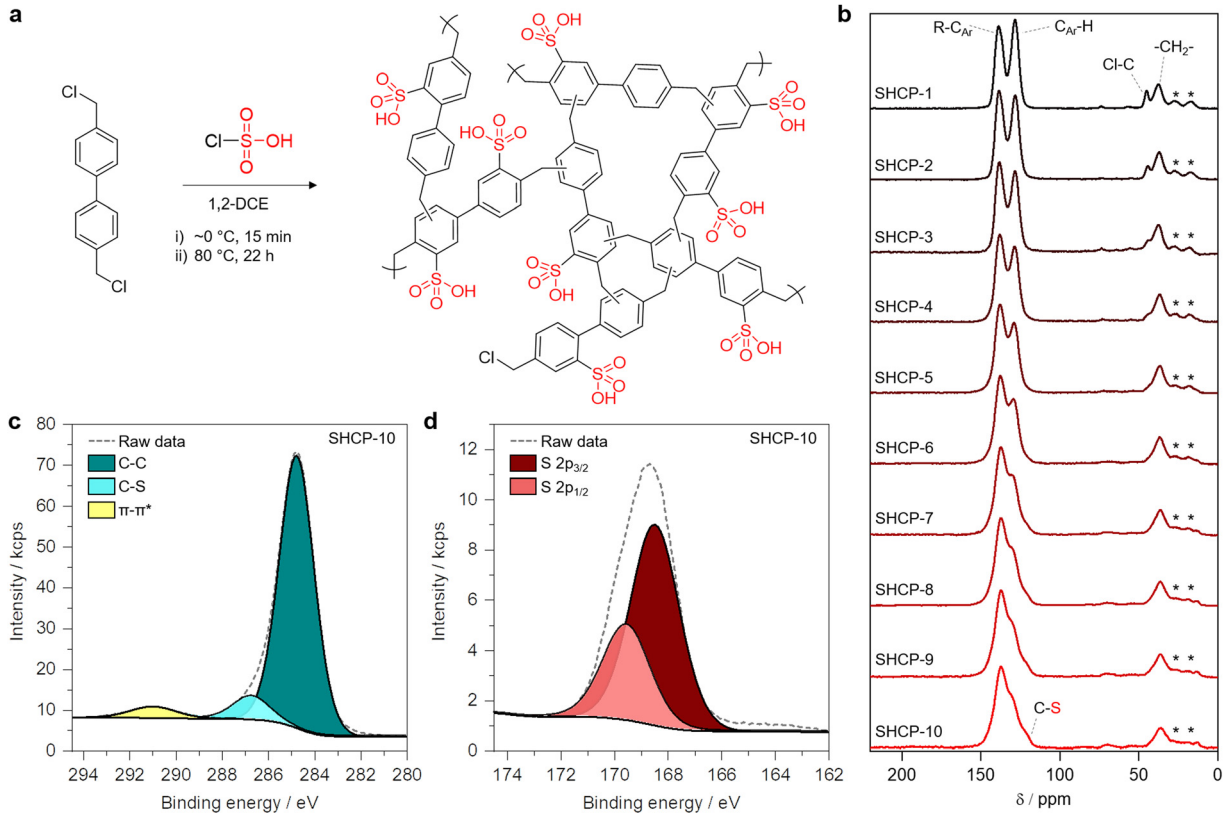

Fig. 1 Sulfonated hypercrosslinked polymer characterisation. (a) Reaction scheme for the one-pot synthesis of SHCPs. (b) ^{13}C CP/MAS solid state NMR spectra for all SHCPs, with increasing catalyst to monomer ratio used in the production of SHCP-1–SHCP-10. * Represents spinning side bands. (c) X-Ray photoelectron C 1s spectrum for SHCP-10. (d) X-Ray photoelectron S 2p spectrum for SHCP-10. (grey dotted lines in (c and d) represent raw data).

polymer formation and sulfonation using Fourier-transform infrared spectroscopy (Fig. S2, ESI†). There, the presence of bands assigned to both SO_3H and C–S bonds emerged with increasing ratios of catalyst to monomer, confirming increasing sulfonation. The diminishing of the C–Cl band across the series was also observed, in good agreement with ssNMR.

Table 1 Summary of SO_3H content and textural properties of SHCPs produced from various ratios of catalyst to monomer, including BET specific surface area, SSA_{BET}, volume of micropores, V_{MICRO}, and total pore volume, V_{TOT}

Sample	Catalyst : monomer (molar ratio)	SO_3H content[a] (mmol g^{-1})	SSA_{BET}[b] (m^2 g^{-1})	V_{MICRO}[b] (cm^3 g^{-1})	V_{TOT}[b] (cm^3 g^{-1})
SHCP-1	0.125	0.03 ± 0.02	539 ± 123	0.11 ± 0.03	0.37 ± 0.07
SHCP-2	0.25	0.44 ± 0.06	899 ± 165	0.14 ± 0.01	0.72 ± 0.19
SHCP-3	0.5	1.15 ± 0.06	1059 ± 165	0.20 ± 0.01	0.77 ± 0.16
SHCP-4	0.75	1.72 ± 0.08	947 ± 89	0.21 ± 0.01	0.60 ± 0.09
SHCP-5	1	2.20 ± 0.13	889 ± 44	0.22 ± 0.01	0.51 ± 0.04
SHCP-6	1.5	2.82 ± 0.09	805 ± 50	0.20 ± 0.00	0.44 ± 0.04
SHCP-7	2	3.24 ± 0.16	723 ± 31	0.20 ± 0.00	0.38 ± 0.02
SHCP-8	2.5	3.40 ± 0.12	706 ± 24	0.20 ± 0.01	0.37 ± 0.01
SHCP-9	3	3.60 ± 0.17	682 ± 14	0.19 ± 0.01	0.36 ± 0.02
SHCP-10	4	3.76 ± 0.11	688 ± 47	0.20 ± 0.01	0.37 ± 0.04

[a] Determined by elemental analysis. [b] Determined from N_2 sorption isotherms at 77 K.

We used X-ray photoelectron spectroscopy (XPS) to gain a more in-depth understanding of SHCPs' chemical compositions (XPS derived quantitative data for all polymers is provided in Table S1, ESI†). The main component of the high-resolution C 1s spectra observed at a binding energy of 284.8 eV is attributed to C–C bonding, encompassing both sp2 aromatic carbon and sp3 carbon in methylene crosslinks (SHCP-10 shown in Fig. 1c). A peak of lower intensity is observed at 286.8 eV, corresponding to C–S. A broad, low intensity π–π* shake-up feature is also observed at 291 eV. High resolution S 2p spectra showed a typical asymmetric peak for a sulfonic acid moiety (SHCP-10 shown in Fig. 1d). The peaks at binding energies of 168.5 eV and 169.5 eV are assigned to S 2p$_{3/2}$ and 2p$_{1/2}$, respectively.[31] This peak is present throughout all sulfonated networks, confirming the vast majority of the sulfur present exists in sulfonic acid groups. Further evidence for this is provided by a consistent ratio of 1 : 3 for S to O across all samples, as would be expected for sulfonic acid groups. Increasing catalyst to monomer ratios led to higher concentrations of sulfonic acid sites in the networks, reaching a maximum sulfur content of 4.6 mmol g^{-1} in SHCP-10, as determined by XPS. This is amongst the highest degrees of sulfonation reported for hypercrosslinked polymers, with another similarly high example reported for carbazole based networks (3.7 mmol g^{-1}, as determined by elemental analysis).[25] Equivalent SHCPs prepared *via* a

two-step conventional approach reported by James *et al.* reached good sulfonation densities of 3.3 mmol g^{-1},[29] however roughly 10 times more chlorosulfonic acid was required than in the synthesis of networks with similar acid densities herein (3.4 mmol g^{-1} in SHCP-8). We hypothesize that polymerisation occurs more rapidly than sulfonation in our approach, leading to the uniform distribution of chlorosulfonic acid throughout the HCP structure. This dispersion facilitates excellent acid densities throughout networks upon sulfonation, as it eliminates the need for the sulfonation agent to permeate into a pre-formed structure.

We employed CHNS-O elemental analysis (EA) to measure the bulk chemical composition of the networks (Table S2, ESI†). The EA results showed a similar trend to XPS, with sulfonation densities increasing upon an increase in catalyst-to-monomer ratio, confirming a good dispersion of acid-sites both at the surface and throughout the bulk of the networks. At higher catalyst-to-monomer ratios (≥ 2), the EA results deviate quite significantly from XPS, with SHCP-10 measured as containing 3.8 mmol g^{-1} of SO_3H compared to 4.6 mmol g^{-1} in XPS. Although this difference may be due in part to variance between bulk and surface concentrations of sulfonate groups, it is likely also due to water adsorption in networks with higher sulfonation densities, prior to EA analysis. This can be observed in the S : O atomic ratios calculated from EA, which ideally should be 1 : 3 but are as high as 1 : 5.4 in SHCP-10, leading to an underestimation of S content. Furthermore, XPS cannot consider H when determining at% of elements present, leading to a slight overestimation. Therefore, the real concentration of SO_3H likely lies somewhere between the values determined by XPS and EA.

In order to probe the hydrophobicity/hydrophilicity across the SHCP networks, we analysed the hygroscopic behaviour of SHCP-1, SHCP-5 and SHCP-10 using dynamic vapour sorption (DVS) (Fig. S3, ESI†). The dry networks were exposed to 90% relative humidity (RH) at 25 °C for 24 h and their water uptake monitored. The least sulfonated network, SHCP-1, exhibited an uptake of 4 wt%, while SHCP-5 and SHCP-10 increased by 77 and 81 wt%, respectively. The dramatic increase in hygroscopicity is attributed to the increased sulfonation densities.

We measured N_2 sorption isotherms for all SHCP polymers at 77 K to gain information about their porous properties (Fig. 2a and Fig. S4, ESI†). The sulfonated networks showed excellent reproducibility regarding their porous properties. Networks displayed characteristics of both Type I and Type IVa isotherms, with uptake at low relative pressures signalling microporosity and significant hysteresis observed upon desorption deriving from capillary condensation, indicative here of mesoporosity/macroporosity. All SHCPs displayed H2 type hysteresis curves, indicative of broad pore size distributions with narrow pore necks.[32] The absence of a closed hysteresis loop is common in the isotherms of HCPs and likely due to the swelling of the networks during adsorption.[33] With increasing sulfonation density the hysteresis loops upon desorption appear less pronounced, indicating that the mesopore component of the networks decreases. This is reflected in the values for total pore volume, V_{TOT}, and micropore volume, V_{MICRO} (Fig. 2b and Table 1), which confirmed the broad pore size distribution. Intriguingly, the micropore volume remains relatively constant with increasing degrees of sulfonation from SHCP-3 onward, permitting the careful control of micropore-to-mesopore/macropore ratio in SHCPs.

The BET specific surface area (SSA_{BET}) of all SHCPs was >530 m^2 g^{-1} (Table 1), with SHCP-1 displaying the lowest SSA_{BET} of 539 m^2 g^{-1}. A trend can be seen across the catalyst set, with SSA_{BET} increasing dramatically to a maximum of 1059 m^2 g^{-1} in SHCP-3 before gradually decreasing to 688 m^2 g^{-1} in SHCP-10. A clear trade-off between porous properties and sulfonation density was observed. In SHCP-1 and SHCP-2, inefficient hypercrosslinking occurs due to the relatively low catalyst to monomer molar ratios, as evidenced by C–Cl in ssNMR and the presence of higher concentrations of residual Cl in XPS (Table S1, ESI†). Although SHCP-3 displays

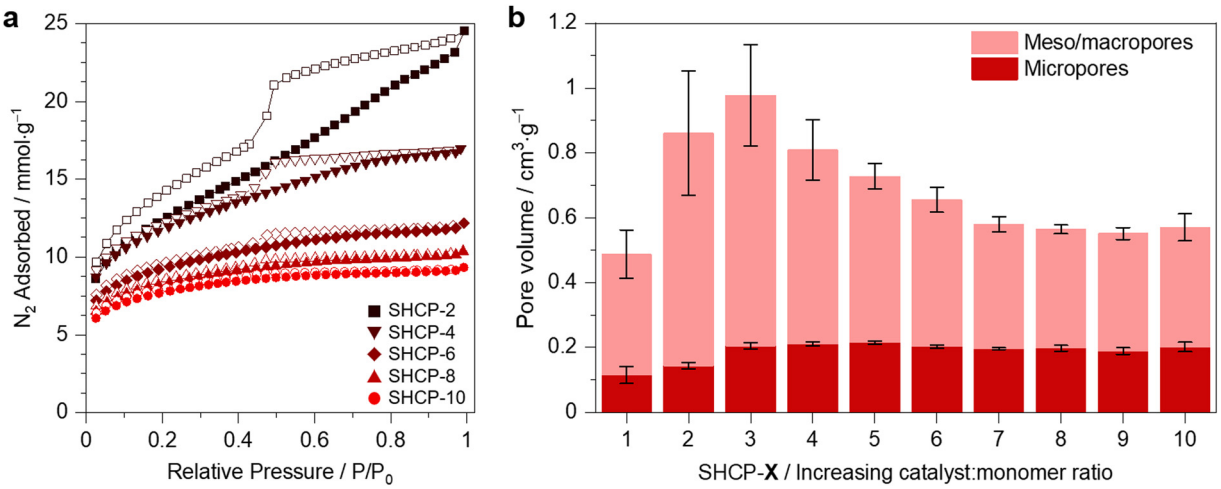

Fig. 2 Textural properties of SHCPs: (a) N_2 adsorption–desorption isotherms for a selection of SHCPs, the remainder are shown in Fig. S4 (ESI†). Filled symbols represent adsorption and empty symbols represent desorption. (b) Pore volume of all SHCPs divided into micropore contributions (red) and mesopore/macropore contributions (pink).

the highest SSA_{BET} of the set, some evidence of remaining C–Cl was again seen during characterisation. It is likely that the degree of sulfonation is insufficient to become significantly detrimental to the porous properties. In previous examples, the self-condensation of 4,4′-bis(chloromethyl)biphenyl catalysed using triflic acid yielded HCPs with SSA_{BET} of up to 1842 $m^2\ g^{-1}$, much higher than the approach herein.[15] However, the production of SHCP-3 requires just one third the amount of acid catalyst used therein. When further increasing the chlorosulfonic acid concentration, as in SHCP-4 to SHCP-10, the resulting SSA_{BET} worsen due to the increased sulfonation. Even with the trade-off between SSA_{BET} and acidity, these materials have excellent porous properties considering their high sulfonation density. The carbazole-based SHCP with a comparable SO_3H concentration of 3.7 mmol g^{-1} displayed a SSA_{BET} of just 346 $m^2\ g^{-1}$.[25] Equivalent SHCPs with sulfonation densities of 3.3 mmol g^{-1} prepared *via* a two-step conventional approach displayed SSA_{BET} of 580 or 850 $m^2\ g^{-1}$, dependent on initial polymerisation catalyst selection.[29]

We analysed the thermal stability of all SHCPs using thermogravimetric analysis (TGA) in either an inert N_2 atmosphere (Fig. 3a and Fig. S5, ESI†) or in air (Fig. S6, ESI†). Negligible weight loss is observed in SHCP-1 and SHCP-2 until >250 °C. With increasing sulfonation density the weight loss prior to and during an isothermal step at 110 °C increases dramatically, reaching a maximum of 21 wt% for SHCP-10, indicative of a significant increase in water adsorption at high sulfonation densities. XPS measurements showed that the chemical composition of the networks remained unchanged after heating overnight at 120 °C under N_2 flow, confirming degradation was not responsible for the weight loss seen in the TGA (Table S1, ESI†). TEM images of SHCP-1, SHCP-5 and SHCP-10 show particles in the micrometer range consisting of fused spherical polymer particles of >100 nm in diameter (Fig. S7, ESI†), in good agreement with similar HCP examples.[13,23] Finally, we employed powder X-ray diffraction (PXRD) to confirm the amorphous nature of all networks (Fig. S8, ESI†).

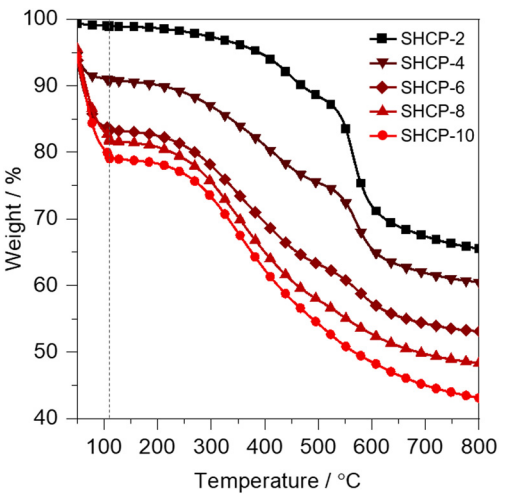

Fig. 3 Thermogravimetric analysis of SHCPs heated to 800 °C in a N_2 atmosphere. A 10 min isothermal step was included at 110 °C to remove residual water (indicated by the vertical grey dotted line).

The synthetic approach to SHCPs described herein provides a set of acidic non-soluble networks in which the sulfonation density, hydrophilicity, and textural properties can be carefully controlled. This presents a unique opportunity for the application of such a set of materials to acid-catalysed conversions in order to unveil optimal catalyst properties. To investigate the catalytic ability of SHCPs, the organic-aqueous biphasic liquid hydrolysis of cyclohexyl acetate to cyclohexanol was selected as a model reaction (reaction scheme in Table 2 and mechanism in Fig. S9, ESI†). We investigated substrate conversion and selectivity across our SHCP series (Table 2). Briefly, SHCP was added to a two-phase cyclohexyl acetate and water system, which was heated at 120 °C under autogenous pressure for 3 h. The reaction products were extracted using ethyl acetate and analysed using gas chromatography-mass spectrometry (GC-MS). A complete set of GC traces are shown in Fig. S10 (ESI†). It is worth noting that all catalysis reactions were repeated at least four times.

Network SHCP-1 showed no measurable catalytic activity due to low acidity (S content of 0.1 mmol g^{-1}). Control experiments with non-acidic hypercrosslinked polymer equivalents confirmed that no measurable conversion was achieved without sulfonation. The more acidic SHCP-2 (S content of 0.4 mmol g^{-1}) gave substrate conversions of 31% with a high standard deviation of ± 18%, suggesting that this polymer lies at a critical concentration upon which catalytic activity depends highly on network acidity. The remaining SHCPs all achieved ≥59% conversion of cyclohexyl acetate, outperforming both the commercial resin Amberlyst-15 and homogeneous (liquid) H_2SO_4.[26] Interestingly, high acid densities did not appear crucial for catalyst performance (Fig. 4). SHCP-3 contained just 1.15 mmol g^{-1} of SO_3H sites and achieved a substrate conversion of 68 ± 8%. Catalytic conversion reached a maximum of 75 ± 2% in SHCP-5 and with increasing sulfonate content (*i.e.* SHCP-6 to SHCP-10), catalytic conversion decreased, reaching 59 ± 8% in SHCP-10, with a SO_3H

Table 2 Catalytic performance of SHCPs in the hydrolysis of cyclohexyl acetate to cyclohexanol. Materials are compared with sulfuric acid and the commercial resin Amberlyst-15

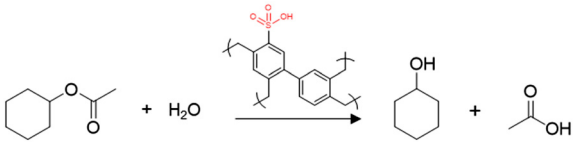

Catalyst	Conversion[a] (mol%)	Selectivity[a] (mol%)
SHCP-1	0	>99
SHCP-2	31 ± 18	>99
SHCP-3	68 ± 7	>99
SHCP-4	72 ± 6	>99
SHCP-5	75 ± 2	>99
SHCP-6	72 ± 5	>99
SHCP-7	64 ± 7	>99
SHCP-8	68 ± 6	>99
SHCP-9	65 ± 7	>99
SHCP-10	59 ± 8	>99
H_2SO_4[b]	27	87
Amberlyst-15[b]	48	95

[a] Determined by GC-MS. [b] Reported in ref. 26.

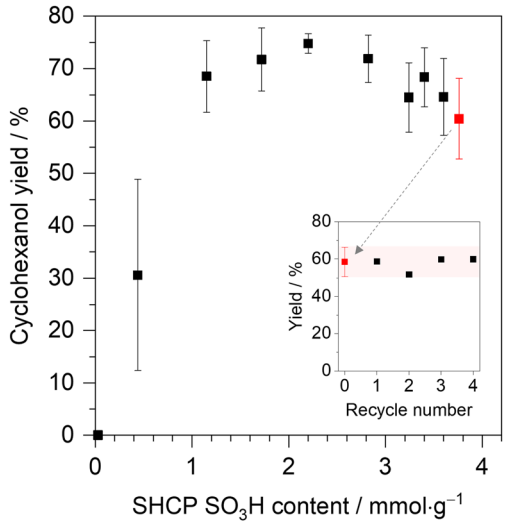

Fig. 4 Cyclohexanol yield of SHCP catalysed hydrolysis of cyclohexyl acetate as a function of SO_3H content. The inset shows the catalytic performance of recycled SHCP-10 in the same conversion over four cycles.

concentration of 3.8 mmol g^{-1}. This emphasises the importance of other catalyst properties as well as acidity for this conversion. During catalytic conversion, networks SHCP-5 to SHCP-8 formed quasi-stable emulsions, demonstrating amphiphilicity by interfacial stabilisation (ESI,† Fig. S11 shows photographs of each network in the biphasic cyclohexyl acetate/cyclohexanol and water system post-catalytic conversion). As the reaction is comprised of both an organic and aqueous phase, the formation of emulsions improves the dispersion of one phase throughout the other and ensures that the catalyst resides at the organic/aqueous interface. Additionally, improved mesopore/macropore content ratios in SHCP-3–SHCP-5 may provide good phase transfer ability, while their high surface areas ensure the substrate good access to active sites, improving conversions compared to materials with reduced mesopore/macroporosity. Selectivity in all materials was >99% for cyclohexanol, with the formation of some trace quantities of cyclohexanone in many examples. We suspect that cyclohexanone is produced *via* oxidation of cyclohexanol, however as this was not confirmed it is herein considered a trace product, which was never found in quantities of >1%. The combination of amphiphilicity, high surface area, hierarchical porosity, and acidity endows SHCP-5 with the highest catalytic ability for the hydrolysis of cyclohexyl acetate to cyclohexanol.

To investigate catalyst stability, we recovered SHCP-5, one of the best performing catalysts, post-cyclohexyl acetate conversion for re-analysis. EA and XPS confirmed no sulfur leaching or significant chemical change after catalyst recovery, demonstrating chemical stability (Tables S3 and S4, ESI†). A slight increase in O was measured in EA but is attributed to the presence of adsorbed moisture. TGA also showed no significant change in thermal stability post-catalysis (Fig. S12, ESI†).

Given the good network stability, we demonstrated the recyclability of SHCP catalysts using SHCP-10 as a representative sample. Post-conversion, the reaction mixture was extracted twice with ethyl acetate before the catalyst network was separated from the reaction mixture by centrifugation. The polymer was washed *via* three centrifugation and redispersion cycles in deionised water and then directly redeployed in the following cyclohexyl acetate conversion. The following conversions were performed under the same initial conditions and the catalyst performance analysed (Fig. 4, inset). Network SHCP-10 showed excellent recyclability across four catalytic cycles with no apparent drop in performance, achieving conversions of 58 ± 4%.

Conclusion

We present a rapid one-pot method for the synthesis of polymeric solid acid catalysts with carefully controlled properties using a dual polymerisation catalyst and sulfonation agent. Ten SHCPs were prepared with varying porous properties, acidity, and hydrophilicity by simply varying the initial catalyst to monomer ratio. These materials could be obtained in less than 24 h by combining the polymerisation and sulfonation steps into a one-pot procedure, significantly increasing the speed and ease of production. This had several advantages over conventional techniques, such as eliminating the need for metal-based polymerisation catalysts, dramatically reducing the amount of toxic solvents and sulfonation agents required, and hence lowering the cost of porous heterogeneous solid-acid catalysts. Comparison with equivalent materials produced *via* conventional routes showed that the properties obtained in SHCPs herein are superior with respect to both acidity and surface area. The SHCPs were applied to the acid-catalysed hydrolysis of cyclohexyl acetate to cyclohexanol. Conversions of up to 75% were measured, with all networks displaying excellent selectivity (>99%). Catalyst recycleability was demonstrated and no significant reduction in catalytic performance was observed over 5 cycles. Results strongly suggested that acidity is only one of a number of important properties in the design of solid acid catalysts, with high acid densities even leading to reduced conversion rates. The ability to fine-tune polymer catalysts allows for the identification of key properties for further catalyst design and optimisation. We envision the application of such polymers to a plethora of acid-catalysed reactions in order to find catalyst properties most suited to each conversion, paving the way to truly tailorable low-cost acid catalysts.

Conflicts of interest

There are no conflicts of interest to declare.

Acknowledgements

The authors acknowledge the funding support of the University of Vienna (Austria). We thank Mina Ghorbanzadeh and Peter Unteregger for assistance with catalyst recycling experiments. We also thank Mag. Johannes Theiner for assistance with elemental analysis, Ing. Alexander Prado-Roller for assistance

with PXRD, and Asst.-Prof. Hanspeter Kählig for assistance with ssNMR.

References

1 P. T. Anastas and J. C. Warner, *Green chemistry: Theory and practice*, Oxford University Press: New York, 1998, 30.
2 L.-B. Sun, X.-Q. Liu and H.-C. Zhou, Design and fabrication of mesoporous heterogeneous basic catalysts, *Chem. Soc. Rev.*, 2015, **44**, 5092–5147, DOI: 10.1039/C5CS00090D.
3 S. Hübner, J. G. de Vries and V. Farina, Why does industry not use immobilized transition metal complexes as catalysts?, *Adv. Synth. Catal.*, 2016, **358**(1), 3–25, DOI: 10.1002/adsc.201500846.
4 M. Rose, Nanoporous polymers: Bridging the gap between molecular and solid catalysts?, *ChemCatChem*, 2014, **5**(6), 1166–1182, DOI: 10.1002/cctc.201301071.
5 C. S. Diercks and O. M. Yaghi, The atom, the molecule, and the covalent organic framework, *Science*, 2017, **355**(6328), 923–931, DOI: 10.1126/science.aal1585.
6 J.-S. M. Lee and A. I. Cooper, Advances in conjugated microporous polymers, *Chem. Rev.*, 2020, **120**(4), 2171–2214, DOI: 10.1021/acs.chemrev.9b00399.
7 L. Tana and B. Tan, Hypercrosslinked porous polymer materials: Design, synthesis, and applications, *Chem. Soc. Rev.*, 2017, **46**, 3322–3356, DOI: 10.1039/C6CS00851H.
8 B. Li, R. Gong, W. Wang, X. Huang, W. Zhang, H. Li, C. Hu and B. Tan, A new strategy to microporous polymers: Knitting rigid aromatic building blocks by external cross-linker, *Macromolecules*, 2011, **44**(8), 2410–2414, DOI: 10.1021/ma200630s.
9 S. L. Wang, C. X. Zhang, Y. Shu, S. L. Jiang, Q. Xia, L. J. Chen, S. B. Jin, I. Hussain, A. I. Cooper and B. E. Tan, Layered microporous polymers by solvent knitting method, *Sci. Adv.*, 2017, **3**(3), e1602610, DOI: 10.1126/sciadv.1602610.
10 A. Krusenbaum, S. Grätz, S. Bimmermann, S. Hutsch and L. Borchardt, The mechanochemical Scholl reaction as a versatile synthesis tool for the solvent-free generation of microporous polymers, *RSC Adv.*, 2020, **10**, 25509–25516, DOI: 10.1039/D0RA05279E.
11 J.-S. M. Lee, T. Kurihara and S. Horike, Five-minute mechanosynthesis of hypercrosslinked microporous polymers, *Chem. Mater.*, 2020, **32**(18), 7694–7702, DOI: 10.1021/acs.chemmater.0c01726.
12 C. D. Wood, B. Tan, A. Trewin, H. Niu, D. Bradshaw, M. J. Rosseinsky, Y. Z. Khimyak, N. L. Campbell, R. Kirk, E. Stöckel and A. I. Cooper, Hydrogen storage in microporous hypercrosslinked organic polymer networks, *Chem. Mater.*, 2007, **19**(8), 2034–2048, DOI: 10.1021/cm070356a.
13 R. T. Woodward, The design of hypercrosslinked polymers from benzyl ether self-condensing compounds and external crosslinkers, *Chem. Commun.*, 2020, **56**, 4938–4941, DOI: 10.1039/D0CC01002B.
14 S. Hou, S. Razzaquea and B. Tan, Effects of synthesis methodology on microporous organic hyper-cross-linked polymers with respect to structural porosity, gas uptake performance and fluorescence properties, *Polym. Chem.*, 2019, **10**, 1299–1311, DOI: 10.1039/C8PY01730A.
15 K. Schute and M. Rose, Metal-free and scalable synthesis of porous hyper-cross-linked polymers: Towards applications in liquid-phase adsorption, *ChemSusChem*, 2015, **8**(20), 3419–3423, DOI: 10.1002/cssc.201500829.
16 L. Prince, P. Guggenberger, E. Santini, F. Kleitz and R. T. Woodward, Metal-free hyper-cross-linked polymers from benzyl methyl ethers: A route to polymerization catalyst recycling, *Macromolecules*, 2021, **54**(19), 9217–9222, DOI: 10.1021/acs.macromol.1c01332.
17 R. T. Woodward, L. A. Stevens, R. Dawson, M. Vijayaraghavan, T. Hasell, I. P. Silverwood, A. V. Ewing, T. Ratvijitvech, J. D. Exley, S. Y. Chong, F. Blanc, D. J. Adams, S. G. Kazarian, C. E. Snape, T. C. Drage and A. I. Cooper, Swellable, water-and acid-tolerant polymer sponges for chemoselective carbon dioxide capture, *J. Am. Chem. Soc.*, 2014, **136**(25), 9028–9035, DOI: 10.1021/ja5031968.
18 V. Rozyyev, D. Thirion, R. Ullah, J. Lee, M. Jung, H. Oh, M. Atilhan and C. T. Yavuz, High-capacity methane storage in flexible alkane-linked porous aromatic network polymers, *Nat. Energy*, 2019, **4**, 604–611, DOI: 10.1038/s41560-019-0427-x.
19 R. Vinodh, C. V. V. M. Gopi, V. G. R. Kummara, R. Atchudan, T. Ahamad, S. Sambasivam, M. Yi, I. M. Obaidat and H.-J. Kim, A review on porous carbon electrode material derived from hypercross-linked polymers for supercapacitor applications, *J. Energy Storage*, 2020, **32**, 101831, DOI: 10.1016/j.est.2020.101831.
20 Y. Gu, S. U. Son, T. Li and B. Tan, Low-cost hypercrosslinked polymers by direct knitting strategy for catalytic applications, *Adv. Funct. Mater.*, 2021, **31**(12), 2008265, DOI: 10.1002/adfm.202008265.
21 K. Dong, J. Zhang, W. Luo, L. Su and Z. Huang, Catalytic conversion of carbohydrates into 5-hydroxymethyl furfural over sulfonated hyper-cross-linked polymer in DMSO, *Chem. Eng. J.*, 2018, **334**, 1055–1064, DOI: 10.1016/j.cej.2017.10.092.
22 J. Zhang, K. Dong, W. Luo and H. Guan, Catalytic upgrading of carbohydrates into 5-ethoxymethylfurfural using SO3H functionalized hyper-cross-linked polymer based carbonaceous materials, *Fuel*, 2018, **234**, 664–673, DOI: 10.1016/j.fuel.2018.07.060.
23 G. E. M. Schukraft, R. T. Woodward, S. Kumar, M. Sachs, S. Eslava and C. Petit, Hypercrosslinked polymers as a photocatalytic platform for visible-light-driven CO_2 photoreduction using H_2O, *ChemSusChem*, 2021, **14**, 1720–1727, DOI: 10.1002/cssc.202002824.
24 S. Wang, M. Xu, T. Peng, C. Zhang, T. Li, I. Hussain, J. Wang and B. Tan, Porous hypercrosslinked polymer-TiO_2-graphene composite photocatalysts for visible-light-driven CO_2 conversion., *Nat. Commun.*, 2019, **10**, 676, DOI: 10.1038/s41467-019-08651-x.
25 S. Bhunia, B. Banerjee and A. Bhaumik, A new hypercrosslinked supermicroporous polymer, with scope for sulfonation, and its catalytic potential for the efficient synthesis of

biodiesel at room temperature, *Chem. Commun.*, 2015, **51**, 5020–5023, DOI: **10.1039/C4CC09872B**.

26 Y. Lei, M. Zhang, G. Leng, C. Ding and Y. Ni, SO_3H-functionalized porous organic polymer with amphiphilic and swelling properties: A highly efficient solid acid catalyst for organic transformations in water, *Microporous Mesoporous Mater.*, 2020, **299**, 110110, DOI: **10.1016/j.micromeso.2020.110110**.

27 A. Stephenson, B. Li, L. Chen, R. Clowes, M. E. Briggs and A. I. Cooper, Efficient separation of propane and propene by a hypercrosslinked polymer doped with Ag(I), *J. Mater. Chem. A*, 2019, **7**, 25521–25525, DOI: **10.1039/C9TA07510K**.

28 Y. Xiong, R. T. Woodward, D. Danaci, A. Evans, T. Tian, H. Azzan, M. Ardakani and C. Petit, Understanding trade-offs in adsorption capacity, selectivity and kinetics for propylene/propane separation using composites of activated carbon and hypercrosslinked polymer, *Chem. Eng. J.*, 2021, **426**, 131628, DOI: **10.1016/j.cej.2021.131628**.

29 A. M. James, S. Harding, T. Robshaw, N. Bramall, M. D. Ogden and R. Dawson, Selective environmental remediation of strontium and cesium using sulfonated hyper-cross-linked polymers (SHCPs), *ACS Appl. Mater. Interfaces*, 2019, **11**(25), 22464–22473, DOI: **10.1021/acsami.9b06295**.

30 G. Xiong, Q. Zhang, B. Ren, L. You, F. Ding, Y. He, X. Fan, N. Wang and Y. Sun, Highly efficient and selective adsorption of cationic dyes in aqueous media on microporous hyper crosslinked polymer with abundant and evenly dispersed sulfonic groups, *ChemistrySelect*, 2020, **5**, 6541–6546, DOI: **10.1002/slct.202000927**.

31 M. Matsuda, K. Funabashi, H. Yusa and M. Kikuchi, Influence of functional sulfonic acid group on pyrolysis characteristics for cation exchange resin, *J. Nucl. Sci. Technol.*, 1987, **24**(2), 124–128, DOI: **10.1080/18811248.1987.9735785**.

32 M. Thommes, K. Kaneko, A. V. Neimark, J. P. Olivier, F. Rodriguez-Reinoso, J. Rouquerol and K. S. W. Sing, Physisorption of gases, with special reference to the evaluation of surface area and pore size distribution (IUPAC Technical Report), *Pure Appl. Chem.*, 2015, **87**, 1051–1069, DOI: **10.1515/pac-2014-1117**.

33 S. Bilodeau, J. Florek and F. Kleitz, Reassessing the physicochemical properties of ordered mesoporous polymer and copolymer nanocasts, *Chem. Ing. Tech.*, 2021, **93**(6), 916–928, DOI: **10.1002/cite.202000238**.